International Journal of Chemical, Materials and Biomolecular Sciences
ISSN: 2415-6620
Vol:4, No:5, 2010

Effects of Formic Acid on the Chemical State and Morphology of As-synthesized and Annealed ZnO Films

Chueh-Jung Huang, Chia-Hung Li, Hsueh-Lung Wang, Tsun-Nan Lin

Abstract**—**Zinc oxide thin films with various microstructures were grown on substrates by using HCOOH-sols. The reaction mechanism of the sol system was investigated by performing an XPS analysis of as-synthesized films, due to the products of hydrolysis and condensation in the sol system contributing to the chemical state of the as-synthesized films. The chemical structures of the as-synthesized films related to the microstructures of the final annealed films were also studied. The results of the Zn $2p_{3/2}$, C 1s and O1s XPS patterns indicate that the hydrolysis reaction in the sol system is strongly influenced by the HCOOH agent. The results of XRD and FE-SEM demonstrated the microstructures of the annealed films are related to the content of hydrolyzed zinc hydrate (Zn-OH) species present, and that content of the Zn-OH species in the sol system increases the HCOOH adding, and these Zn-OH species existing in the sol phase are responsible for large ZnO crystallites in the final annealed films.

Keywords**—**zinc oxide, hydrolysis catalyst, zinc acetate source, formic acid.

I. Introduction

MUCH attention has been focused on the preparation of zinc oxide thin films by wet sol techniques in recent years because the wet sol process is more cost effective and convenient for mass production [1]-[3]. Some literatures have reported that characteristics of the wet sol's ZnO films are influenced by processing parameters, such as type of dopant [4]-[7], strength of reagent [8]-[10], and annealing temperature [11]-[12]. Various syntheses have been carried out by changing the parameters to prepare particular morphologies of ZnO films for special applications, e.g. the films having smooth surface are suitable for high conductivity electrodes [13]-[14], whereas the films having a rougher surface could be used for optical devices or sensors [15]-[16].

The basic principle of the wet sol method for the synthesis of the ZnO film involves the evolution of inorganic polymer chains (condensed zincoxane chain (-(Zn-O)$_x$-)) through the reaction of hydrolysis and condensation of zinc sources and the formation of a colloid solution in the reaction system [17]-[19]. The hydrolysis reaction of the zinc source can occur without the addition of an external catalyst, whereas it can be significantly enhanced when some catalysts are employed. Variant acid- or base agents have been used as hydrolysis catalysts to promote the hydrolysis of the zinc source in the sol system [20]-[21]. However, the effect of the zinc source's hydrolysis on the structure and morphology of the ZnO films are still inadequately understood.

Very recently, we found that the microstructures of ZnO films are strongly influenced by the pH values of the precursor sol [22]. The aim of the present work is to further investigate how the mechanism of the acid catalyst affects the reaction condition of the sol system, by paying special attention on the effect of the acid agent on the chemical state of the as-synthesized films and final annealed films. And the chemical bonding and microstructure of these prepared films were investigated by XRD, XPS and FE-SEM.

Authors are with the Department of Chemical Engineering , Hsiuping Institute of Technology, Taichung 412, Taiwan
e-mail:cjhcyy@ms57.hinet.net; hcj@mail.hit.edu.tw

II. Experimental

1. Synthesis of as-synthesized and annealed ZnO thin films

The raw solution consists of a 3 ml of 1 M zinc acetate dihydrate ($Zn(CH_3COO)_2{\cdot}2H_2O$, as a zinc source) ethanol solution and a 10 ml of 10 wt% polyvinyl alcohol (PVA, as a tackifier). An acid hydrolysis agent, e.g. formic acid (HCOOH), was added into the raw solution until the pH value of the solution reaching 0.5. And the mixture was allowed to reacted at 60 ^oC for 12 h to yield an acidic precursor sol. Then the synthesized sols were deposited on glass substrates (coring 2870) using a spin-coating method with a rotating speed at 1500 rpm for 60 s. After each coating, the samples were dried in an oven at 100 ^oC for 10 min, and the procedures from spin-coating to drying were repeated three times, thus as-synthesized films were obtained. Finally, the as-synthesized films were annealed in air at 500 ^oC for 1.5 h to crystallize.

2. Characterization of the films

The crystal structure of the films was examined by glancing incidence X-ray diffraction (GIXD) (MacScience MXP3 X-ray diffractometer), which was operated at 40 kV and 150 mA using Cu K_α radiation. The surface morphology and cross-section structure of the films were observed using a field emission scanning electron microscopy (FE-SEM), JEOL JSM-6700F, operated at 3.0 kV. The chemical composition of the films was analyzed using X-ray photoelectron spectroscopy (XPS), ULVAC-PHI 5000, combined with 4 keV Ar^+ sputter depth profiling. A standard X-ray source, 15kV, 25W, Al K_α (hv=1486.6 eV) was used. Binding energies were referenced to the C_{1s} peak at 284.8 eV.

III. Results and Discussion

1. XRD analysis

The crystal structure of the films was examined by XRD analysis. The XRD spectra of the as-synthesized and annealed films are shown in Figure 1. Fig. 1a and b show the XRD spectra of the as-synthesized films prepared with raw-sol (without adding HCOOH agent) and HCOOH-sol, respectively. And it can be seen that no diffraction peaks appeared for the as-synthesized films. However, the films show a crystalline ZnO phase with a hexagonal wurtzite structure after 500 ^{o}C annealing treatment. For the annealed films, three main peaks of the (100), (002) and (101) planes with small peaks of the (102) and (110) planes were observed in the XRD pattern, as shown in Fig. 1c and d.

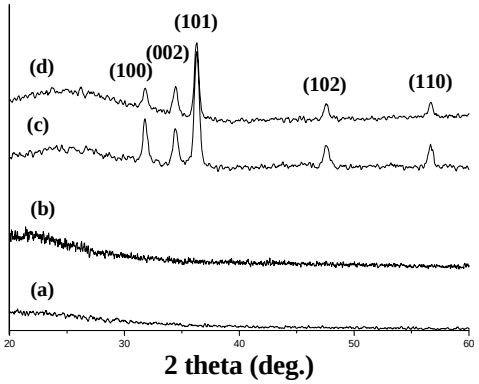

Fig. 1. XRD spectra of as-synthesized films prepared with raw-sol (a), and HCOOH-sol (b), and annealed films prepared with raw-sol (c), and HCOOH-sol (d).

2. Zn $2P_{3/2}$ XPS

XPS analysis was employed to understand the chemical state of the as-synthesized films. Figure 2 displays the Zn $2P_{3/2}$ XPS spectra of the as-synthesized films. Theoretically, the Zn $2P_{3/2}$ pattern of the Zn-O oxide bond is at 1021.8 eV, whereas the shift of the peak position is generally observed while the changing in chemical environment of the Zn^{2+} ions [23]-[24]. Therefore, for both the as-synthesized films in Fig. 2, the binding energy peak located at 1022.0 eV corresponds to the condensed zincoxane (-(Zn-O)$_x$-)) bonds, and which indicates that the reaction of hydrolysis and condensation of zinc acetate has been conducted. However, the presence of the other higher binding energy component, zinc species(ZnR), located at 1022.7 eV suggests that the acetate Zn (Zn-$OCOCH_3$) groups or hydrated Zn (Zn-OH) groups also exist in the films.

3. C 1s XPS

The zinc species, un-hydrolyzed Zn-$OCOCH_3$ or hydrolyzed Zn-OH groups, can be further distinguished by the detailed C 1s core level patterns. Fig. 3a shows the deconvolution of C 1s pattern of the film prepared with the raw precursor sol. The C 1s line consists of three peaks at 284.6, 286.6 and 289.5 eV, which corresponds to the C-C/C-H, C-OH and O-C=O bonds [23]-[24], respectively. The C-C/C-H and C-OH components are contributed by the sol system, including the tackifier PVA and the zinc source. The presence of the O-C=O component indicates that the Zn-$OCOCH_3$ groups of the zinc acetate source are not completely hydrolyzed or converted.

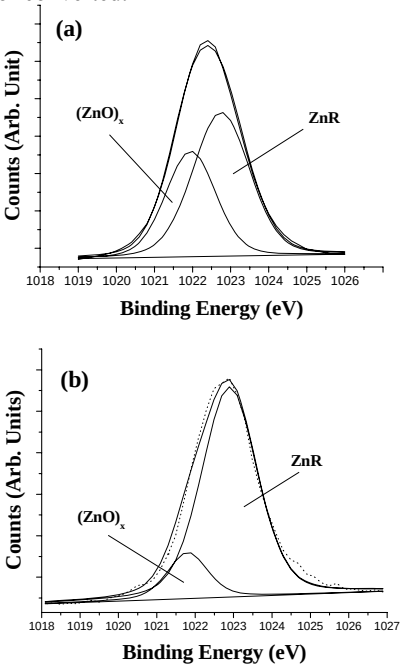

Fig. 2. Zn 2P3/2 core-level spectra of the as-synthesized films: (a) raw-sol, and (b) HCOOH-sol.

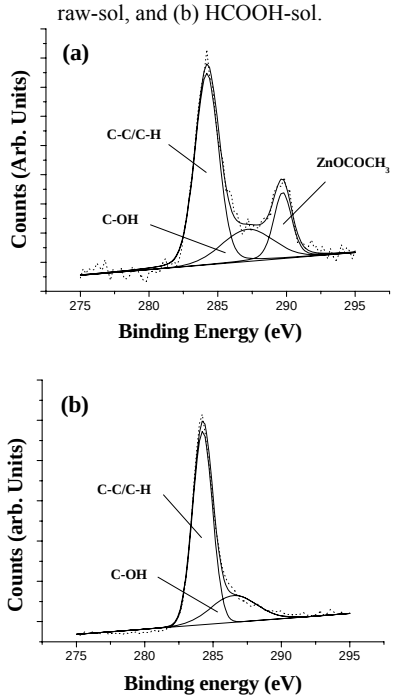

Fig. 3. C 1s core-level spectra of the as-synthesized films: (a) raw-sol, and (b) HCOOH-sol.

In addition, as shown in Fig. 3b, after adding the HCOOH into the precursor sol, the C 1s profile of the film was altered, and the content of the O-C=O component significantly disappeared. This result indicates that the Zn-$OCOCH_3$ groups of the sol system were completely converted during the hydrolysis and condensation reaction. The result also reveals that the Zn $2P_{3/2}$ peaks located at 1022.7 eV, shown in Fig. 2, are contributed primarily by the Zn-OH groups in the sol system.

4. O 1s XPS

Furthermore, the detailed O 1s XPS patterns of the as-synthesized films are shown in Fig. 4. The O 1s patterns of the raw precursor sol's film is deconvoluted into four peaks, Fig. 4a, the lowest energy located at 529.7 eV corresponds to (-$(Zn\text{-}O)_x$-)) bonds, and other peaks located at 530.5, 531.5 and 532.2 eV corresponds to Zn-$OCOCH_3$, Zn-OH and C-OH bonds [23]-[24], respectively. It can be observed that after HCOOH acid was employed, as shown in Fig. 4b, the Zn-OH contents of the film increase, however, the Zn-$OCOCH_3$ contents of the films disappeared. The content of the (-$(Zn\text{-}O)_x$-)), Zn-OH and Zn-$OCOCH_3$ components for the prepared films are listed in Table I.The k_1 and k_2 in Table I represent the reaction rate constant of hydrolysis and condensation, respectively. As the detailed O 1s data of the as-synthesized films, the relative ratio k_1/k_2 is calculated using consecutive first-order reaction formula and the results are also given in Table I. Table I depicts that the k_1/k_2 ratio of the HCOOH-sol system was larger than that of the raw sol system (k_1/k_2 ratio 0.29). This result indicates that the added HCOOH causes an increase in the hydrolysis rate more quickly than the condensation rate in the acid sol system.

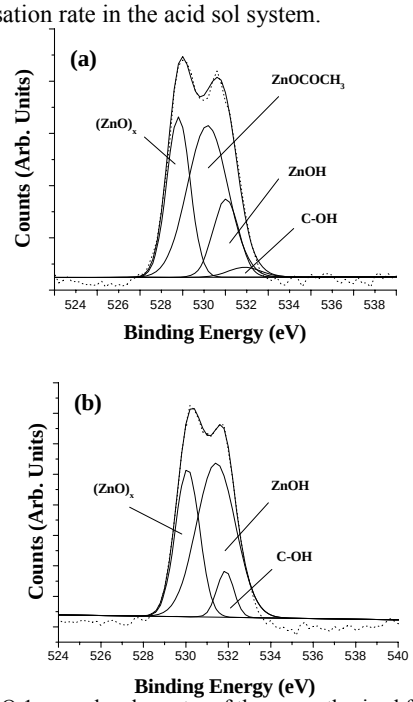

Fig. 4. O 1s core-level spectra of the as-synthesized films: (a) raw-sol, and (b) HCOOH-sol.

TABLE I
Relative peak area fractions of the zinc species (-$(Zn\text{-}O)_x$-, Zn-OH and Zn-$OCOCH_3$) of the as-synthesized films and the k_1/k_2 ratio of the sol system calculated by O 1s XPS data

Samples	peak area fraction (%)			k_1/k_2 ratio[a]
	-$(Zn\text{-}O)_x$-	Zn-$OCOCH_3$	Zn-OH	
Raw-sol	31.5	51.6	16.9	0.29
HCOOH-sol	37.0	--	63.0	k1>> k2

a: $k_1$and k_2 determined using consecutive first-order reaction formula.

5. Reaction of hydrolysis and condensation

As the results of the Zn $2P_{3/2}$, C 1s and O 1s analysis, the sol reaction of the zinc source can be suggested in Fig. 5. The hydrolysis reaction of the zinc acetate (structure I), through the addition of water, replaces acetate groups ($OCOCH_3$) with hydroxyl groups (OH) forming hydrolyzed Zn bonds (structure II). The condensation reaction involving the zinc hydrate or zinc acetate groups produces polymer zincoxane chains (structure III) plus the by products, water or acetate acid.

6. XPS analysis of annealed films

The chemical bonding of the ZnO crystallites, the XPS analysis of the annealed films prepared with raw-sol, and HCOOH-sol was also performed. Figure 6a shows the Zn $2P_{3/2}$ XPS spectrum of the raw-sol's film, and the XPS spectrum of the film can be deconvoluted into two peaks, higher binding energy peak at 1021.8 eV corresponding to perfect ZnO bonds, whereas lower binding energy peak (ZnO') at 1020.8 eV indicating the presence of deficient ZnO states. In addition, it was observed that the peak content of the prefect ZnO bonds (1021.8 eV) of the HCOOH-sol's films, as shown in Fig. 6b, is larger than that of the raw-sol's film. This indicates that the crystal structure and the bonding state in the ZnO crystallites have become better after employing the acid agent.

7. FE-SEM analysis

Fig. 7a-b shows the images of the raw-sol's film after annealing treatment, and the morphology of the annealed raw-sol's film exhibits a surface with small and round-like crystallites, and the particle size is about ~20 nm.

However, it can be seen that on the surface of the annealed HCOOH-sol's film appears large crystallites with particle size about 500~ 1000 nm, and some of the large crystallites display a hexagonal geometry, as shown in Fig. 7c-d.

In further considering the influence of the HCOOH hydrolyisi agent on the chemical state of the as-synthesized film, as the numbers of the zinc hydrate (Zn-OH) species increased with the HCOOH adding, it is believed that the hydrogen bonds increase and drive the hydrolyzed species to jointly aggregate in the sol system. In addition, as the high content of the aggregated zinc hydrate species causes to produce the large ZnO crystallites during the annealing process at high temperature by direct dehydration.

IV. Conclusions

ZnO thin films were prepared using raw-sol and HCOOH-sol, respectively. The results of the XRD and FE-SEM analyses reveal that the microstructure and the surface morphology of the final annealed ZnO films is strongly influenced by the HCOOH agent. And the detailed XPS analysis of the Zn $2P_{3/2}$, C 1s and O 1s core level spectra of the as-synthesized films indicate the reaction state of the system's hydrolysis was enhanced by the acid agent. It was also found that the initial k_1/k_2 ratio, without HCOOH adding, of the sol system is 0.29, indicating that hydrolysis is slower than the condensation reaction. However, the hydrolysis in the sol system was promoted by adding the HCOOH agent. The content of the zinc-acetate ($Zn\text{-}OCOCH_3$) groups decreased as the HCOOH being used, and the numbers of the zinc hydrate (Zn-OH) species increase. These ZnOH species are responsible for the large ZnO crystallites of the annealed films.

References

[1] J. Bao, Z. Liu, Y. Zhang, and N. Tsubaki, Catal. Commun., 9, 913 (2008).
[2] X. Zhou, T. Jiang, J. Zhang, X. Wang, and Z. Zhu, Sensor. Actua. B, 123, 299 (2007).
[3] H. Matsui, H. Saeki, H, Tabata, and T. Kawai, J. Electrochem. Soc., 150 (9), G508 (2003).
[4] J. H. Lee, and B. O. Park, Thin Solid Films, 426, 94 (2003).
[5] M. Izaki, and Y. Saijo, J. Electrochem. Soc., 150 (2), C73 (2003).
[6] M. Izaki, and J. Katayama, J. Electrochem. Soc., 147 (1), 210 (2000).
[7] K. Sakurai, T. Kubo, D. Kajita, T. Tanabe, H. Takasu, and S. Fujita, Jap. J. Appl. Phys., Patr 2, 39, L1146 (2000).
[8] K. Yu, Z. G. Jin, X. Liu, J. Zhao, and J. Y. Feng, Appl. Surf. Sci., 253, 4072 (2007).
[9] M. de la L. Olvera, H. Gómez, and A. Maldonado, Sol. Energy Mater. Sol. Cells, 91, 1449 (2007).
[10] M. Yang, D. J. Wang, Y. H. Lin, Z. H. Li, and Q. L. Zhang, Mater. Chem. Phys., 88, 333 (2004).
[11] S. Q. Chen, J. Zhang, X. Feng, X. H. Wang, L. Q. Luo, Y. L. Shi, Q. S. Xue, C. Wang, J. H. Zhu, and Z. Q. Zhu, Appl. Surf. Sc., 241, 384 (2005).
[12] L. Znaidi, G. J. A. A. Soler Illia, S. Benyahia, C. Sanchez, and A. V. Kanaev, Thin Solid Films, 428, 257 (2003).
[13] Y. H. Cheng, L. K. Teh, Y. Y. Tay, H. S. Park, C. C. Wong, and S. Li, Thin Solid Films, 504, 41 (2006)
[14] J. Puetz, F. N. Chalvet, and M. A. Aegerter, Thin Solid Films, 442, 53 (2003).
[15] T. Du, and O. J. Ilegbusi, J. Mater. Sci., 39, 6105 (2004).
[16] J. H. Lee, K. H. Ko, and B. O. Park, J. Cryst. Growth, 247, 119 (2003).
[17] C. D. Bojorge, H. R. Cánepa, U. E. Gilabert, D. Silva, E. A. Dalchiele, and R. E. Marotti, J. Mater. Sci.: Mater. Electron., 18, 1119 (2007).
[18] K. M. Lin, and P. J. Tsai, Mater. Sci. Eng. B, 139, 81 (2007).
[19] M. Ortega-López, A. Avila-García, M. L. Albor-Aguilera, and V. M. S. Resendiz, Mater. Res. Bullet., 38, 1241 (2003).
[20] L. Armelao, M. Fabrizio, S. Gialanella, and F. Zordan, Thin Solid Films, 394, 90 (2001).
[21] M. de la L. Olvera, A. Maldonado, R. Asomoza, O. Solorza, and D. R. Acosta, Thin Solid Films, 394, 242 (2001).
[22] C. J. Huang, M. C. Chiu, H. C. Yao, D. C. Tsai, and F. S. Shieu, J. Electrochem. Soc. 155 (12), K211 (2008).
[23] G. Machado, D. N. Guerra, D. Leinen, J. R. Ramos-Barrado, R. E. Marotti, and E. A. Dalchiele, Thin Solid Films, 490, 124 (2005).
[24] C. J. Huang, J. J. Lin, and F. S. Shieu, Jpn. J. Appl. Phys., 44 (8) 6332 (2005).

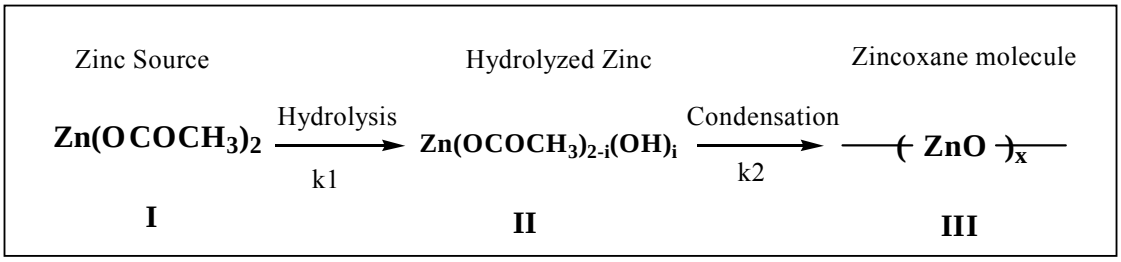

Fig. 5. A Schematic diagram illustrating the reaction of the sol system

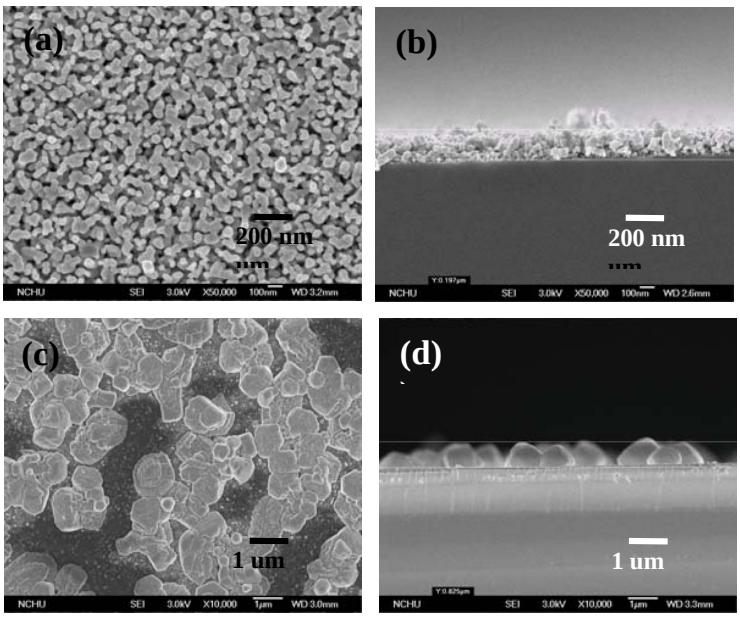

Fig. 7. FE-SEM images of plan-view and cross-section of the annealed films prepared with raw-sol (a), and HCOOH-sol